High-resolution x-ray spectrometer based on spherically bent crystals for investigations of femtosecond laser plasmas

Cite as: Review of Scientific Instruments **69**, 4049 (1998); https://doi.org/10.1063/1.1149249
Submitted: 09 June 1998 • Accepted: 07 August 1998 • Published Online: 02 December 1998

B. K. F. Young, A. L. Osterheld, D. F. Price, et al.

High-resolution x-ray spectrometer based on spherically bent crystals for investigations of femtosecond laser plasmas

B. K. F. Young, A. L. Osterheld, D. F. Price, R. Shepherd, and R. E. Stewart
Lawrence Livermore National Laboratory, Livermore, California 94551

A. Ya. Faenov, A. I. Magunov, T. A. Pikuz, and I. Yu. Skobelev
Multicharged Ions Spectra Data Center of VNIIFTRI, Mendeleevo, Moscow region, 141570 Russia

F. Flora, S. Bollanti, P. Di Lazzaro, and T. Letardi
ENEA, Dipartimento Innovazione, Settore Fisica Applicata, 00044 Frascati, Rome, Italy

A. Grilli
INFN Frascati, 00044 Frascati, Rome, Italy

L. Palladino and A. Reale
Dipartamento di Fisica e INFN g.s. INGS, Universita de L.Aquila, 67010 L'Aquila, Italy

A. Scafati and L. Reale
Instituto Sup. Di Sanita, Roma e INFN sez Sanita, 00040 Rome, Italy

(Received 9 June 1998; accepted for publication 7 August 1998)

Ultrashort-pulse, laser-produced plasmas have become very interesting laboratory sources to study spectroscopically due to their very high densities and temperatures, and the high laser-induced electromagnetic fields present. Typically, these plasmas are of very small volume and very low emissivity. Thus, studying these near point source plasmas requires advanced experimental techniques. We present a new spectrometer design called the focusing spectrometer with spatial resolution (FSSR-2D) based on a spherically bent crystal which provides simultaneous high spectral ($\lambda/\Delta\lambda \approx 10^4$) and spatial resolution ($\approx 10\ \mu$m) as well as high luminosity (high collection efficiency). We described in detail the FSSR-2D case in which a small, near point source plasma is investigated. An estimate for the spectral and spatial resolution for the spectrometer is outlined based on geometric considerations. Using the FSSR-2D instrument, experimental data measured from both a 100 fs and a nanosecond pulse laser-produced plasma are presented. © *1998 American Institute of Physics.* [S0034-6748(98)00712-6]

I. INTRODUCTION

The x-ray spectroscopy of multicharged ions has been a useful tool for investigating the atomic kinetics and radiation properties of dense plasmas generated using high-powered, short-pulse lasers of 100 fs to 10 ps duration (for example, see Refs. 1–15). Recent experiments have shown that these ultrashort-pulse laser-produced plasmas are of very small volumes and are very high density and highly nonstationary. The x-ray spectra are very complex and require high-resolution spectroscopic instrumentation with very high collection efficiencies.

The x-ray emission spectra from 100 fs plasmas have often been measured using flat crystal or von Hamos type spectrometers.[2–15] The von Hamos design provides increased collection efficiency with good resolving power over traditional flat crystal instruments. Recently, simultaneous high spectral ($\lambda/\Delta\lambda \approx 10^4$) and high spatial ($\approx 10\ \mu$m) resolution spectra from a 100 fs ultrashort-pulse laser-produced plasma was measured using a focusing spectrometer with spatial resolution (FSSR-1D) based on a spherically bent crystal with a large open aperture and small radius of curvature.[16–28] The advantages of such instruments are high spectral and spatial resolution as well as high luminosity due to the use of spherically bent crystals.

The FSSR-1D spectrometer design utilizes both the focusing aspects of the spherical mirror configuration as well as the Bragg crystal x-ray diffraction and must satisfy both conditions simultaneously. To satisfy the spherical mirror focusing properties, the distance between the source, the spherical mirror (crystal), and the object plane (film or other x-ray detector) must be related as

$$1/a + 1/b = 1/f, \tag{1}$$

where a is the distance between the source and the mirror, b is the distance between the mirror and detector, and f is the focal length of the spherical mirror. In the case of the FSSR-1D spectrometer, the x-ray detector must be placed on the Rowland circle for optimal spectral resolution (analogous to the classical Johann type scheme for cylindrically bent crystal spectrometers). It follows that for obtaining spatial resolution perpendicular to the dispersion plane, the source must be set up at the distance

$$a = R\ \cos\ \varphi/\cos 2\varphi \tag{2}$$

from the crystal and the detector must be located at a distance

$$b = R\ \cos\ \varphi \tag{3}$$

from the crystal, where R is the radius of curvature of the spherically bent crystal, φ is the angle of incidence (from normal incidence) of the incoming radiation and is related to the usual Bragg angle as $\varphi = 90° - \theta_B$ (the Bragg equation is $m\lambda = 2d \sin \theta_B$, where d is the interplanar spacing of the crystal and m is the diffraction order of the crystal). It is clear from Eq. (2) that the incident angle φ cannot be greater than 45° and the distance a increases very quickly with increasing angle φ. This condition strictly limits the range of usable angles available for the FSSR-1D spectrometer design. This limitation is further compounded by the small number of x-ray diffraction crystals available for use in the small radius of curvature, spherically bent crystal design (i.e., mica and some quartz crystal orientations) and only partly mitigated due to the great number of useable diffraction (reflection) orders for the mica crystal.

A variation of the spherical crystal spectrometer design is based on placing the x-ray detector outside of the Rowland circle (the FSSR-2D scheme[16–17,29]). Typically, the large plasma source size drastically reduces the spectral resolution and the FSSR-2D configuration is usually used for monochromatic imaging of the plasma.[20–33] For ultrashort-pulse laser-produced plasmas and in particular, 100 fs duration laser pulses, the plasma size is very small (typically <10 μm) and the FSSR-2D configuration can be used to obtain high-resolution spectra. In this article, we consider in detail, the possibility of using spherically bent crystals in the FSSR-2D configuration to measure x-ray spectra from 100 fs laser-produced plasmas with simultaneously high spectral and high spatial (perpendicular) resolution. Experimental results, obtained using such high-luminosity instruments are presented for 100 fs and nanosecond laser-produced plasmas.

II. GEOMETRICAL MODELING OF FSSR-2D SCHEME

In this article, we only consider the role the plasma source plays in the spectral resolution of the FSSR-2D spectrometers and present the geometrical modeling for the dispersion (meridinal) plane for spherically bent crystals. The positions of the source, crystal, and detector are determined by the geometric optic equation [Eq. (1)] perpendicular to the dispersion (saggital) plane of the spherically bent crystal. Consider that in the dispersion plane, the x-ray emission source is placed at the distance a from the center of the crystal surface at an angle of incidence φ (with respect to normal to the crystal surface), corresponding to the Bragg diffraction angle $\theta_B = 90° - \varphi$ for wavelength λ. In the FSSR-2D scheme (see Fig. 1), the position of the spectral line relative to the center of the crystal sphere is determined by

$$f = \frac{R \sin \varphi}{\sin \gamma}, \tag{4}$$

where R is the crystal radius of curvature. γ is the angle between the direction from the detector to the center of the emission source and the reflected ray and is given by

$$\gamma = \pi - 2\varphi - \sin^{-1}\left(\frac{R \sin \varphi}{s}\right), \tag{5}$$

with $s = (R^2 + a^2 - 2Ra \cos \varphi)^{1/2}$ as the distance from the source to the center of the crystal sphere.

Now consider the displacement of the line image on the detector due to the finite source size r. Only the case for $a > R$ is considered which is most applicable for investigations of 100 fs laser-produced plasmas. Rotating the triangle SCF (see Fig. 1) to match the source bordering along FS, one obtains

$$s \pm r = \frac{R \sin \varphi}{\cos(\beta + \delta_\pm)}, \tag{6}$$

where $\sin \beta = (a - R \cos \varphi)/s$, $\delta_\pm$ is the rotation angle with $(\pm)$ corresponding to the $(+)$ clockwise and the $(-)$ counterclockwise directions. In the case $r \ll s$,

$$\delta_\pm = \delta = \frac{r}{s} \cot \beta. \tag{7}$$

The positions of the spectral line corresponding to the source border are

$$f^\pm = \frac{R \sin \varphi}{\sin(\gamma \mp \delta)}. \tag{8}$$

Using this relationship, the total image bandwidth can be written as follows:

$$\Delta f_s = f^- - f^+ = 4R \sin \varphi \left(\frac{\cos \gamma \sin \delta}{\cos 2\delta - \cos 2\gamma}\right). \tag{9}$$

On the other hand, the linear dispersion of crystal gives the spectral lines position,

$$\Delta f_\lambda = \left(\frac{df}{d\lambda}\right)_s \Delta\lambda = \left(\frac{df}{d\varphi}\right)_s \left(\frac{d \log \lambda}{d\varphi}\right)^{-1} \frac{\Delta\lambda}{\lambda}, \tag{10}$$

where the derivatives are taken for a fixed s.

From the Bragg reflection law $m\lambda/(2d) = \cos \varphi$, it follows:

$$\left(\frac{d \log \lambda}{d\varphi}\right) = -\tan \varphi. \tag{11}$$

The derivative in Eq. (10) is defined from Eq. (4)

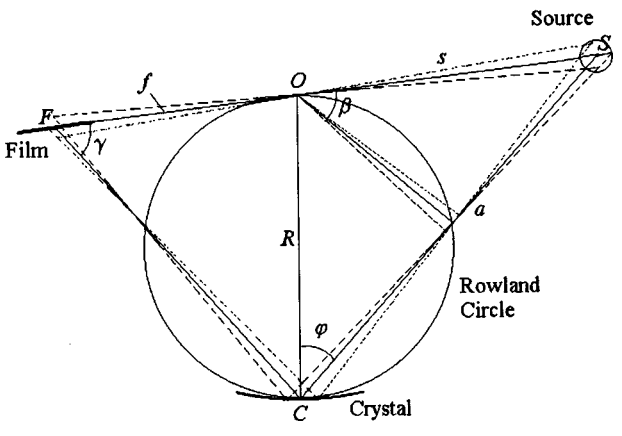

FIG. 1. Schematic of showing the FSSR-2D scheme.

$$\left(\frac{df}{d\theta}\right)_s = R\,\frac{\cos\varphi - \sin\varphi\,\cot\gamma\,(d\gamma/d\varphi)_s}{\sin\gamma}. \tag{12}$$

Equating Eqs. (9) and (10) after substitution Eqs. (11) and (12) one establishes a limitation for spectral resolution from the finite source size with uniform parameters:

$$\left(\frac{\Delta\lambda}{\lambda}\right)_{\min} = \left|A\left(\frac{a}{R},\varphi\right)\right|\,\frac{\sin 2\gamma\,\sin\delta}{\cos 2\delta - \cos 2\gamma}, \tag{13}$$

where

$$A\left(\frac{a}{R},\varphi\right) = \frac{2\left(\frac{a}{R}-\cos\varphi\right)\tan\varphi}{\left(\frac{a}{R}-\cos\varphi\right)\cot\varphi + \left(2\frac{a}{R}-\cot\varphi\right)\cot\gamma}. \tag{14}$$

For $\delta \ll 1$, Eq. (13) can be written in the form

$$\left(\frac{\Delta\lambda}{\lambda}\right)_{\min} = \frac{r}{R}\left|B\left(\frac{a}{R},\varphi\right)\right|, \tag{15}$$

where

$$B\left(\frac{a}{R},\varphi\right) = \frac{2\cos\beta\,\tan\varphi}{\left(\frac{a}{R}-\cos\varphi\right)(\cot\varphi\,\tan\gamma + 1) + a/R}. \tag{16}$$

Let us consider the consequences of Eqs. (15) and (16) for experiments using FSSR-2D spectrometers. Equation (15) shows that a spectral resolution $\Delta\lambda/\lambda \sim 10^{-3}$ requires that the size of source could be estimated from the ratio $r/R \sim 10^{-3}$. In Fig. 2(a), the variation of B is given by Eq. (16) as the distance between the source and the center of crystal surface for several Bragg angles. The variation of B with angle φ for several values of a/R are shown in Fig. 2(b). From Fig. 2, we find that for typical radius of curvature spherical crystals $R \geqslant 100$ mm and the size of x-ray source less than 100 μm for 100 fs laser-produced plasmas, a spectral resolution $\Delta\lambda/\lambda \sim 10^{-3}$ is realized for practically all angles of incidence and distances $a/R > 1$ [see Figs. 2 and 3, where $(\Delta\lambda/\lambda)/(r/R) < 10^0$]. For higher spectral resolution (about 2×10^{-4}) and similar plasma source conditions, Fig. 2 shows the ratio $(\Delta\lambda/\lambda)/(r/R)$ must be 2×10^{-1} for a wide range of incident angles and distances from the plasma. The gaps for curves with $\varphi < \pi/4$ correspond to the FSSR-1D geometry scheme when the film is on the Rowland circle ($\gamma \approx \pi/2$), and for the FSSR-2D case as $B \to 0$ as shown in Eq. (16). This result is well known and means that the spectral resolution for FSSR-1D scheme is not limited by source size. We mention here that we have only considered the geometrical aspects of FSSR-2D scheme for spectral resolution, which might be achieved. The actual experimental spectral resolution must also include contribution due to the width of crystal rocking curve, broadening of spectral lines, etc.

Note that Eq. (15) also gives an estimation of the spatial resolution in the dispersion direction for x-ray line radiation with the relative spectral line width $\Delta\lambda/\lambda$. It follows that if the spectral resolution due to the source size [Eq. (15)] is smaller than the relative emission linewidth, the images of different points inside this region overlap each other. The results for $\Delta\lambda/\lambda = 10^{-3}$ are shown in Figs. 3(a) and 3(b). From Fig. 3, for practically all angles and distances $a/R > 1$, the spatial resolution in the dispersion plane ranges between 50 and 500 μm and is not viable for studying the finite size, 100 fs laser-produced plasmas. This is in contrast to the FSSR-2D spectrometer design where the saggital plane (perpendicular to the dispersion plane) provides micron spatial resolution dependent primarily on optical aberrations of the spherically bent crystal and the accuracy of the spectrometer alignment.

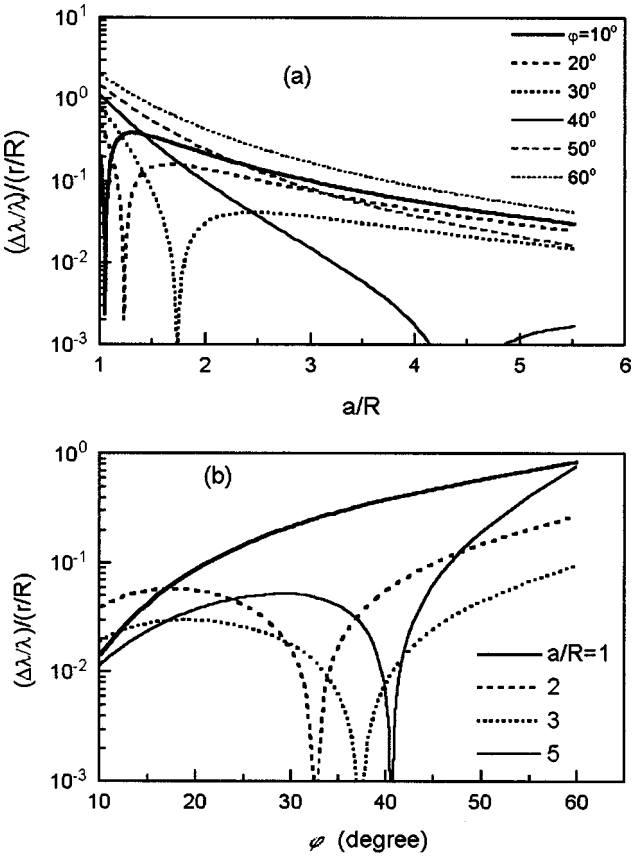

FIG. 2. Estimates of the spectral resolution for a finite size source as described in Eqs. (15) and (16) are graphically shown as functions of a/R (distance between the source and the center of the crystal surface) and the angle of incidence φ (with respect to normal incidence to the crystal).

A geometrical ray-tracing program package has been developed at MISDC to provide a quick estimate of the spectral resolution for the FSSR-1D and FSSR-2D spectrometer configurations.[34] The program calculates the spectral resolution given the size of the plasma source, x-ray wavelengths of interest, the distances a and b between the crystal source and crystal detector, respectively, for different x-ray diffraction crystals, angles of incidence, etc. This ray-tracing program was successfully used to align the FSSR spectrometers used to measure the experimental results presented below.

III. FEMTOSECOND AND NANOSECOND LASER-PRODUCED PLASMA EXPERIMENTS

Two sets of test experiments were conducted to demonstrate the utility of the FSSR spectrometers. The experiments reported here were conducted at the Ultrashort Pulse Laser

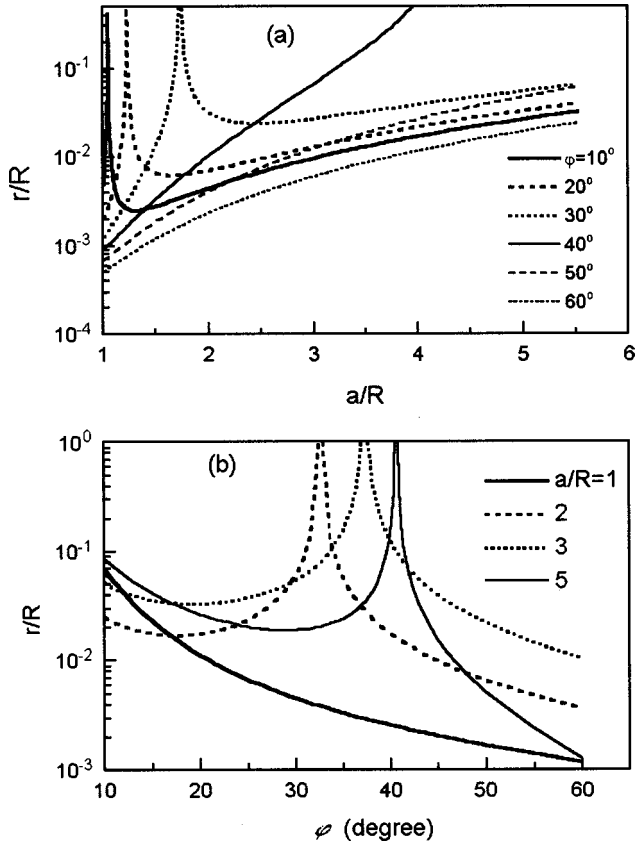

FIG. 3. Estimates of the spatial resolution in the dispersion direction for a spectral linewidth of $\Delta\lambda/\lambda$ as described in Eqs. (15) and (16) are graphically shown as functions of a/R and the angle of incidence φ.

(USP) Facility of Lawrence Livermore National Laboratory[35–37] and at the nanosecond HERCULES Laser Facility of ENEA, Frascati.[38–44] The femtosecond experiments were performed using 130 fs, frequency-doubled Ti:sapphire (400 nm) laser light. The laser energy used for the experiments was about 150 mJ and focused to a diffraction limited spotsize of <4 μm in diameter, producing a peak intensity of 10^{19} W/cm^2. In the second set of experiments, the plasmas were heated by a XeCl laser with wavelength $\lambda=0.308$ nm and pulse duration about 12 ns. The typical energy of a laser pulse was 2 J, focused to a spotsize of diameter 30–70 μm, resulting in a peak intensity $(4-8)\times10^{12}$ W/cm^2. In both cases, the laser radiation was focused on the surface of solid slab (crystal) Si targets. In the Frascati experiments, Mg targets were also used. In both cases, the x-ray emission from the laser-produced plasma was measured using a FSSR-2D spectrometer with spherically bent quartz $(10\underline{1}0)$ crystal, with a radius of curvature of $R=186$ mm. In the Frascati experiments, a FSSR-2D spectrometer with spherically bent mica crystal, with a radius of curvature of $R=150$ mm was also used. The crystal, plasma sources and DEF-2 photographic film were placed according to the FSSR-2D scheme described above.

Images and densitometer traces of spectra measured in vicinity of the Heα Si XIII resonance line are presented in Figs. 4 and 5, for the 100 fs USP and 12 ns HERCULES experiments. In both cases, all parameters of the experimental setup were the same including the distance between crystal and plasma source $a=225$ mm, the distance between crystal and film $b=247.2$ mm, and the angle of incidence $\varphi=37.9°$ (for a quartz $10\underline{1}0$ crystal). The resulting spectral dispersion for the FSSR-2D spectrometer was nearly 0.007 Å/mm. (Note: the distance between the resonance Heα line and j satellite line $1s2p^2\ ^2D_{5/2}-1s^22p\ ^2P_{3/2}$ was about 13.5 mm on the film.) The theoretical spectral resolution obtained by the MISDC ray-tracing package for this geometry was more than $\lambda/\Delta\lambda=6600$ assuming a plasma source size of about 70 μm. Because of the high luminosity of the FSSR-2D spectrometer, high-resolution x-ray spectra (for a film density greater than 1.0 for the Heα resonance line) was recorded using only 13 shots for the 100 fs laser heating case and 60 shots in the nanosecond laser heating case. As shown in Fig. 5, not only are the k, j satellites well resolved as is often seen in nanosecond laser plasma spectra, but satellite lines due to transitions from high-n levels of Li-like ions are also well resolved. Such high-n satellite structures are very closed to the Heα line and are typically not well resolved. Also note that there are clearly differences in the intensities and shape of lines for spectra near the resonance Heα line for the two measured spectra reflecting significant differences in

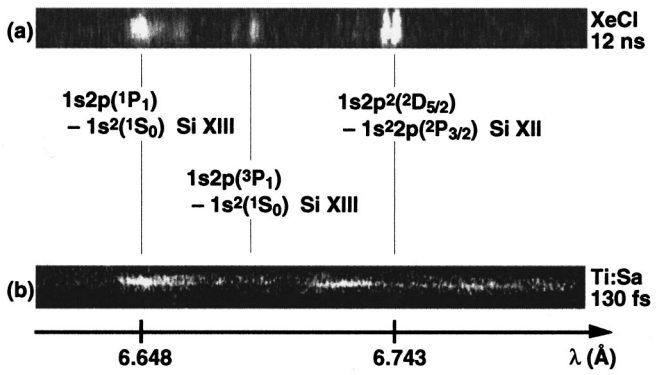

FIG. 4. Images of Si x-ray spectra, in the vicinity of the He$_\alpha$ line: (a) obtained in 12 ns XeCl laser-produced plasma experiments, and (b) obtained in 100 fs Ti:sapphire laser-produced plasma experiments.

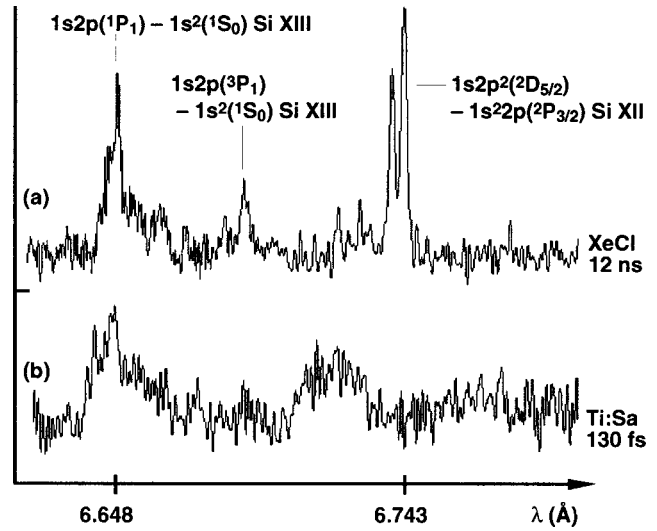

FIG. 5. Densitometer traces of the Si x-ray spectral data shown in Fig. 4 for (a) 12 ns XeCl experiments, and (b) 100 fs Ti:sapphire experiments.

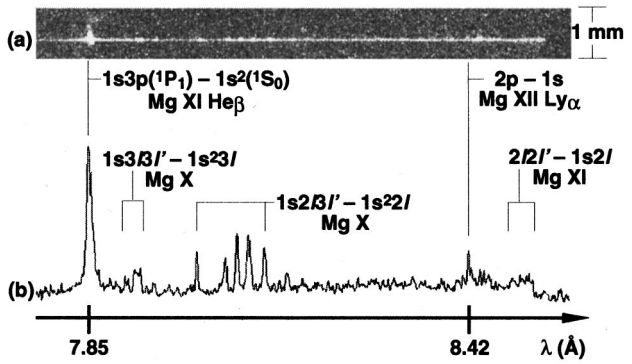

FIG. 6. Mg x-ray spectra including the He_β and Ly_α spectral lines obtained in 12 ns XeCl laser-produced plasmas: (a) spectral image, (b) densitometer trace.

plasma conditions for the 100 fs and 12 ns laser-produced plasmas.

In Fig. 6, the spectral image and densitometer trace of the Mg spectra between Heβ and Lyα of Mg are presented from the HERCULES experiments. This spectrum was obtained in the nanosecond plasma experiments using the FSSR-2D spectrometer with a spherically bent mica crystal with $R=150$ mm (distances a and b were 300 and 133.3 mm, respectively, and the angle of incidence $\varphi=35.7°$). The spectral dispersion in this experiment was 0.039 Å/mm. Ray-trace modeling for this geometry calculated a geometrical spectral resolution better than $\lambda/\Delta\lambda=10^4$ for a plasma source size about 200 μm. The measured Mg spectra shown in Fig. 6, demonstrates how well the FSSR-2D spectrometers can be used to obtain very high spectral resolution data over a reasonably large spectral range. The spectrum shows well-resolved Li-like satellites lines due to transitions between $1s2l3l'-1s^22l$ levels and $1s3l3l'-1s^23l$ satellites for the same Mg XI ion. The wide spectral range of about 0.8 Å also included well-resolved spectra of Lyα (Mg XII) and its satellites. Simultaneously, the data are spatially resolved [see Fig. 6(a)] perpendicular to dispersion plane. The full size of the emitted zone was about 100 μm and spatial resolution in this direction was about 10 μm.

IV. DISCUSSION

We have successfully designed and fielded FSSR-1D and FSSR-2D based on spherically bent crystals with a small radius of curvature as effective tools for studying the x-ray emission spectra from 100 fs laser-produced plasmas or any other point source plasmas. The advantages of such spectrometers include: (1) high luminosity due to the large open aperture and focusing properties of the spherically bent crystals, (2) simultaneously high spectral and spatial resolution perpendicular to the dispersion plane, (3) compact size of the spectrometers which allow them to used in nearly any target chamber, (4) wide spectral range (nearly 1–19.5 Å) coverage using different orientations of quartz crystals, or multiple diffraction orders for mica crystals.

ACKNOWLEDGMENTS

Part of this work was performed under the auspices of the U.S. Department of Energy by the Lawrence Livermore National Laboratory under Contract No. W-7405-Eng-48. Part of this work was supported by the Russian Fundamental Science Foundation under Grant No. 96-02-16111.

[1] F. B. Rosmej *et al.*, J. Quant. Spectrosc. Radiat. Transf. **58**, 859 (1997); T. Kato *et al., ibid.* **58**, 661 (1997).
[2] P. Audebert *et al.*, Europhys. Lett. **19**, 189 (1992).
[3] A. Zigler *et al.*, Phys. Rev. A **45**, 1569 (1992).
[4] G. A. Kyrala *et al.*, Appl. Phys. Lett. **60**, 2195 (1992).
[5] O. Peyrusse *et al.*, J. Phys. B **26**, L511 (1993).
[6] J. C. Kieffer *et al.*, Phys. Fluids B **5**, 2676 (1993).
[7] P. Audebert *et al.*, J. Phys. B **27**, 3303 (1994).
[8] R. C. Mancini *et al.*, J. Phys. B **27**, 1671 (1994).
[9] J. P. Matte *et al.*, Phys. Rev. Lett. **72**, 1208 (1994).
[10] A. Rousse *et al.*, Phys. Rev. E **50**, 2200 (1994).
[11] O. Peyrusse *et al.*, Phys. Rev. Lett. **75**, 3862 (1995).
[12] Z. Jiang *et al.*, Phys. Plasmas **2**, 1702 (1995).
[13] J.-C. Gauthier *et al.*, Phys. Plasmas **4**, 1811 (1996).
[14] R. Shepherd *et al.*, J. Quant. Spectrosc. Radiat. Transf. **58**, 911 (1997).
[15] B. K. F. Young *et al.*, J. Quant. Spectrosc. Radiat. Transf. **58**, 991 (1997).
[16] A. Ya. Faenov *et al.*, Phys. Scr. **50**, 333 (1994).
[17] T. A. Pikuz *et al.*, J. X-Ray Sci. Technol. **5**, 323 (1995).
[18] I. Yu. Skobelev *et al.*, JETP **81**, 692 (1995).
[19] J. Abdallah, Jr., *et al.*, Quantum Electron. **23**, 1005 (1993).
[20] A. Ya. Faenov *et al.*, Phys. Rev. A **51**, 3529 (1995).
[21] J. P. Geindre *et al.*, Phys. Scr. **53**, 645 (1996).
[22] B. A. Bryunetkin *et al.*, J. Quant. Spectrosc. Radiat. Transf. **53**, 45 (1995).
[23] P. V. Nickles *et al.*, JETP Lett. **62**, 927 (1995).
[24] F. B. Rosmej *et al.*, J. Phys. B **29**, L299 (1996).
[25] F. B. Rosmej *et al.*, J. Quant. Spectrosc. Radiat. Transf. **58**, 859 (1997).
[26] A. Ya. Faenov *et al.*, Proc. SPIE **3157**, 10 (1997).
[27] R. Doron *et al.*, Phys. Rev. A **58**, 1859 (1998).
[28] S. A. Pikuz *et al.*, JETP Lett. **66**, 480 (1997).
[29] B. A. Bryunetkin *et al.*, Quantum Electron. **24**, 356 (1994).
[30] V. M. Dyakin *et al.*, Quantum Electron. **24**, 1100 (1994).
[31] S. A. Pikuz *et al.*, Phys. Scr. **51**, 517 (1995).
[32] A. Bartinik *et al.*, Quantum Electron. **25**, 50 (1995).
[33] A. Ya. Faenov *et al.*, Phys. Scr. **53**, 591 (1996).
[34] A. I. Magunov, A. Ya. Faenov, T. A. Pikuz, and I. Yu. Skobelev, Ray-tracing code for focusing spectrographs with spatial resolution (FSSR-1D, -2D), MISDC, VNIIFTRI, 1997.
[35] D. F. Price *et al.*, Phys. Rev. Lett. **75**, 252 (1995).
[36] A. Sullivan *et al.*, Opt. Lett. **21**, 603 (1996).
[37] J. D. Bonlie *et al.*, Proc. SPIE **2116**, 312 (1994).
[38] S. Bollanti *et al.*, Phys. Scr. **51**, 326 (1995).
[39] S. Bollanti *et al.*, J. X-Ray Sci. Technol. **5**, 323 (1995).
[40] S. Bollanti *et al.*, Il Nuovo Cimento **18D**, 1241 (1996).
[41] P. Albertano *et al.*, Proc. SPIE **3157**, 164 (1997).
[42] A. E. Dtepanov *et al.*, J. Quant. Spectrosc. Radiat. Transf. **58**, 937 (1997).
[43] G. A. Vergunova *et al.*, Phys. Scr. **55**, 483 (1997).
[44] F. B. Rosmej *et al.*, JETP Lett. **65**, 708 (1997).